ORIGINAL ARTICLE

Numerical study of three-dimensional detonation structure transformations in a narrow square tube: from rectangular and diagonal modes into spinning modes

Y. Huang · H. Ji · F. Lien · H. Tang

Abstract Three-dimensional (3-D) detonation structure transformations from rectangular and diagonal modes into spinning modes in a narrow square tube are investigated by high-resolution simulation. Numerical simulations are performed with a Riemann solver of the HLLC-type, new cell-based structured adaptive mesh refinement data structure, high-order, parallel adaptive mesh refinement reactive flow code. A simplified one-step kinetic reaction model is used to reveal the 3-D detonation structure. The four different types of initial disturbances applied in the ZND profiles lead to the structures of rectangular in phase, rectangular out of phase, rectangular partial out of phase and diagonal, respectively, during the initial stages of detonation propagation. Eventually, all these detonation structures evolve into the self-sustained spinning detonations. The asymmetric disturbance leads to a stable spinning detonation much faster than the rest. The important features in the formation of spinning detonation are revealed using a 3-D visualization, and a remarkable qualitative agreement with experimental and numerical results is obtained with respect to the transverse wave dynamics and detonation front structures. The transverse wave collisions produce the unburnt gas pockets and the energy to sustain the detonation front propagation and distortion. The periodic pressure oscillation of front plays a complex role as it shifts the reaction zone structure with an accompanying change in the driving energy of transition and the detonation parameters which result in the more distorted front and the unstable detonation. Eventually, the unstable distorted detonation evolves into a spinning detonation.

Y. Huang (✉)
Department of Aeronautics, Xiamen University,
Xiamen, Fujian 361005, China
e-mail: huangyue@xmu.edu.cn

Y. Huang · H. Tang
College of Energy and Power Engineering, Nanjing University
of Aeronautics and Astronautics, Nanjing , Jiangsu 210016, China

H. Ji
Waterloo CFD Engineering Consulting Inc., Waterloo,
ON N2T 2N7, Canada

Y. Huang · F. Lien
Department of Mechanical Engineering, University of Waterloo,
Waterloo, ON N2L 3G1, Canada

1 Introduction

A detonation is a shock-induced supersonic combustion regime which consists of a discontinuous hydrodynamic shock wave supported by an exothermic reaction. All self-sustaining gas phase detonations front exhibits complicated three-dimensional (3-D), time-dependent structures with interior multiple transverse waves [1,2]. The classical detonation front is a wrinkled leading shock, in which the triple point joints the alternate stronger Mach stem, the weak incident wave and the transverse wave. The instabilities of the detonation lead to the development of triple lines along the precursor shock. These triple lines have different transverse velocities and, consequently, collide with each other. The trajectories of the triple lines form the so-called cellular pattern which is the characteristic feature of detonations. The detailed structures and properties of three-dimensional detonation waves have been studied experimentally and numeri-

cally. There have been many advances in the detonation modeling and experimental characterization, and both numerical and experimental studies have revealed that at least three types of structures of detonations can be produced, namely, rectangular, diagonal, and spinning modes [3–7].

Extensive experiments have been carried out in rectangular or square ducts; Strehlow [3] proposed a rectangular mode which was verified by Takai et al. [4]. Hanana et al. [5] have recently shown the existence of the rectangular in phase, rectangular out of phase and diagonal cellular detonation front structures. Lee et al. [6,7] discovered the detail structures of a single-headed spinning mode through detonation experiments in a square duct.

However, due to limitations in obtaining sufficient accurate experimental diagnostic tools, experiment could not clearly substantiate the complete transient flow field of physical and chemical state variables and the 3-D phenomenology of detonation. Numerical simulations thus act as complements to experiments for the study of complex detonation structure. Simulations of planar detonation structures are seen in such simulations (Mach et al. [8], Bourlioux et al. [9], Oran et al. [10], Gamezo et al. [11], Sharpe et al. [12], Hu et al. [13], the latest by Mahmoudi et al. [14] and Kessler et al. [15], as well as in references therein). The majority of two-dimensional unstable detonation simulations present qualitative insights into the cellular detonation and reproduce the transverse wave trajectories observed from experiments. Nevertheless, 3-D detonation structures such as spinning modes and diagonal modes as well as many important features such as slapping waves of the rectangular modes cannot be described in two-dimensional simulations. Moreover, advancements made in numerical algorithms coupled with the rapidly decreasing cost of computation make 3-D simulations a viable approach to explore the detonation structures. Thus, the simulations of 3-D detonation structures [16–26] have been presented in recent years.

3-D detonation simulations in the rectangular duct have been originally performed by Williams et al. [16]. Their simulations showed that a rectangular out of phase structure of detonation front is much more complicated than that of the two-dimensional case. Over the past decade, Tsuboi et al. [16–21] and collaborators have carried out numerous 3-D simulations of the detonation structures in both circular tubes and square tubes, including detailed propagating detonation structures in different detonation modes, detonation front structure and formation of keystone and unburned pockets behind the detonation front. In particular, the spinning detonations have been intensively studied in both circular tubes and square tubes by Tsuboi et al. [19–21]. It has been found out that the transverse detonation plays an important role in the spinning detonation propagation. The rest of the 3-D simulations about detonation have reproduced all experimentally observed types of detonations, namely rectangular in phase, rectangular out

of phase, and diagonal and investigated the detonation front structures [21–26]. Their computation showed the important features of those detonation modes and a good qualitative agreement with the available experimental and numerical data.

Most of the previous 3-D simulations focus on describing the structure of the different types of detonation while few deals with the potential transformations among these detonation modes and the drives of the detonation front evolution. Moreover, the mechanism of onset of the single-head spinning detonation in a narrow duct is not clear. However, a few works on this issue have been conducted by the numerical studies for square tubes. Dou et al. [26] attempted to identify the transformation between a diagonal and a spinning detonation in their 3-D simulations, because of the limited number of cases and the absence of the sufficient resolution; the result cannot be regarded as a conclusive. Besides, there is an absence of the detail about when and why the diagonal mode evolves into a spinning detonation. Therefore, the dynamic evolutions of the detonation flow towards the rectangular or diagonal structures, and transformations from these structures to spinning detonations in a narrow duct are necessary to study through the further computational resolutions as well as the mechanisms of onset of the single-head spinning detonation in a narrow tube.

In this paper, we investigate the 3-D detonation structure transformations from rectangular and diagonal modes into spinning detonations in a narrow square tube, in which the spinning detonations are produced using different types of initial disturbances. Based on the simulation results, the details about when and why the rectangular (in phase, out of phase and partial out of phase) and diagonal structures evolve into the spinning detonations are discussed.

2 Schematic of rectangular, diagonal and spinning detonation structures

Based on the previous numerical and experimental results [5,6,20], here we give the descriptions of the rectangular, diagonal and spinning detonation structures and redraw the schematic of the both structures and the movement of the triple line in a period of a mode cycle as shown in Fig. 1. The rectangular structure is characterized by orthogonal waves travelling independently on the walls of flow domain, by the straight triple lines emanating from the leading front that move parallel to the opposite walls, and by the "slapping wave" exhibiting on the detonation cells (see Fig. 1a, b). The diagonal structures are characterized by the transverse waves moving along the diagonal line of diagonal front, the diagonal triple lines formation on the normal to the diagonal and the absence of the distinct "slapping wave" on the walls as shown in Fig. 1c. A structure is "in phase" means that triple

Fig. 1 Schematic of the typical detonation structures and the movement of the *triple line* in a period of detonation cycle. The *black and gray arrows* represent the Mach stems and incident shock, respectively. *V* and *H* denote for *vertical* and *horizontal* wall, respectively. *V* and *H* are two adjacent walls **a** *rectangular* in-phase mode, **b** *rectangular* out of phase mode, **c** *diagonal* mode, **d** *spinning* mode
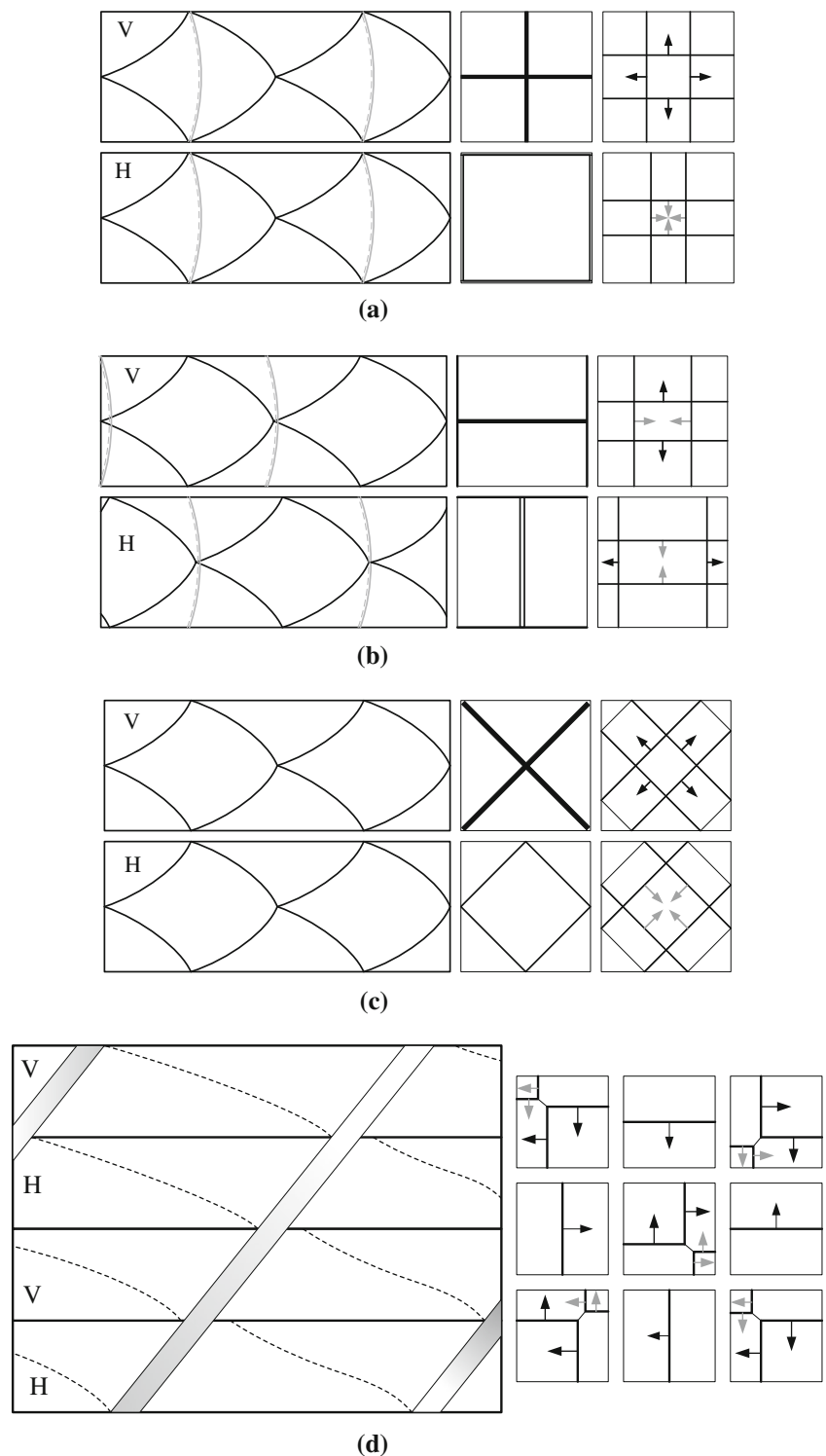
line collisions of the both families of triple line (the apex of the both orthogonal structures) locate in the same duct cross section (Fig. 1a is rectangular in phase); otherwise, it is an "out of phase" structure (Fig. 1b is rectangular out of phase). The single-headed spinning structure in a rectangular duct is composed of a transverse wave rotating around the circumference of the wall, two orthogonal triple lines propagating partial out of phase, a transverse harmonic superimposing on the spinning head and perturbing the circumferential rotary motion [6,20] (see Fig. 1d).

3 Physical and numerical models

3.1 Governing equations and numerical methods

The Euler equations for 3-D unsteady reactive flows were solved numerically. For the sake of simplicity, the chemical reaction is taken as an exothermic irreversible one-step reaction that obeys the Arrhenius law. The unburned and burned gases are assumed as an ideal gas and have the same molecular weights and Lewis numbers. The governing equations can be written as

$$\frac{\partial \rho}{\partial t} + \frac{\partial}{\partial x_j} \left(\rho u_j \right) = 0, \tag{1}$$

$$\frac{\partial \left(\rho u_i \right)}{\partial t} + \frac{\partial}{\partial x_j} \left(\rho u_i u_j + p \delta_{ij} \right) = 0, \tag{2}$$

$$\frac{\partial \left(\rho E \right)}{\partial t} + \frac{\partial}{\partial x_j} \left(u_j \left(\rho E + p \right) \right) = 0, \tag{3}$$

$$\frac{\partial}{\partial t} \left(\rho Z \right) + \frac{\partial}{\partial x_j} \left(\rho u_j Z \right) = -\kappa \rho \left(1 - Z \right) \exp \left(-E_A / RT \right). \tag{4}$$

We consider the gas mixture to be a perfect gas, so that the state equation is

$$p = \rho R T, \tag{5}$$

and the total energy E is given by the formula:

$$E = \frac{p}{\rho \left(\gamma - 1 \right)} + \left(1 - Z \right) q + \frac{1}{2} u_i^2, \tag{6}$$

where ρ denotes density, u_i denotes the component of the velocity in the x_i direction, p is pressure, δ_{ij} denotes Kronecker symbol ($\delta_{ij} = 1$ if $i = j$, and $\delta_{ij} = 0$ otherwise), κ is the pre-exponential factor (frequency factor), E_A is the activation energy for reaction, Z is fuel mass fraction of the products, T is temperature and q is the heat of reaction. The total energy and internal energy are related as $E = e + (u_i u_i)/2$, where e is internal energy.

The thermodynamic and hydrodynamic quantities are non-dimensionalized before solving the above equations, and the non-dimensionalization process is described in [27]. A time-operator splitting approach (or the method of fractional steps) [22,25] and [27] is used to decouple the reactive source term and the hydrodynamic transport term numerically [22,25] and [27]. A high-resolution finite volume discretization is used to achieve a proper upwinding in all fields of flames, shocks, and detonation fronts. The cell-face convective fluxes are calculated by the Harten, Lax, and van Leer with contact restoration (HLLC) approximate Riemann solver. HLLC Riemann solver is extended to a second-order accurate method with MUSCL-type TVD variable extrapolation technique. The semi-discrete formulations of hydrodynamic transport equations are integrated in time using a third-order accurate, three-stage explicit Runge–Kutta scheme.

A new proposed reconstruction method is used for evaluation of the fluxes through the bounding faces of a control volume [27]. To simulate detonation waves in high-resolution within a reasonable amount of computational cost, we employ an adaptive mesh refinement (AMR) method, in which the mesh is dynamically refined at shock waves, flames and detonation fronts. A new cell-based structured adaptive mesh refinement (CSAMR) data structure is employed for implementation and parallelization of our AMR code. Details about the governing equations and numerical algorithms are given in Refs. [25,27]. While studying detonation reacting flows incompatible with the normal detonation, one always has to make sure that the physical instabilities are not numerically driven. The code for reactive Euler flow has been validated for unsteady flows embodied shock wave and detonation wave in 2-D and 3-D [25,27], and the numerical results are in well agreement with various results reported previously in the literature.

3.2 Computational domains and initial conditions

In the following sections, we present the numerical result for transverse wave evolutions in the narrow square tubes, in which we utilize AMR data structure within an implementation of an AMR solver. All computations use the ZND solution as the initial condition, and $\gamma = 1.2$, $E_A = 10$, $q = 50$ and overdriven factor $f \equiv 1.2$ is considered here. The half-reaction length of the ZND profile is used as the reference length $L_{\text{reference}}$ and the reference time $t_{\text{reference}}$ is $L_{\text{reference}} / \sqrt{R T_0}$. Using one-dimensional ZND theory, we can estimate that half-reaction length is about 0.2 mm at initial condition with $p_0 = 1\,\text{kPa}$ and $T_0 = 300\,\text{K}$. The Von Neumann point is placed at $x = 12$ on the computational domain with dimensions of $[0, 24] \times [0, 4] \times [0, 4]$. The 15% pressure increase has been added in a pocket as the initial perturbation to accelerate the growth of the flow instabilities. Figure 1 shows the computational domain and the structures of initial disturbances (Case A, B, C and D) are used to produce rectangular (in phase, out of phase and partial out of phase), and diagonal structures during the initial stages of propagation. The grid resolution was tested initially to maintain high resolution to understand the detailed 3-D structure of the detonation [25]. The adaptive grids have $192 \times 32 \times 32$ cells at the coarsest level and two additional levels of refinement such that the average number of computational cells is about 3,400,000 for all four cases. A constant inflow with $-D_{\text{CJ}}$ is applied at the left, the reflected outflow conditions at the right boundary. The adiabatic and slip wall boundary conditions are used at all other sides.

Fig. 2 Schematic of the structures of the initial perturbation within pockets of 15 % pressure increase and the computational domain. **a** Computational domain, **b** the structures of the initial perturbation


(a)

(b)
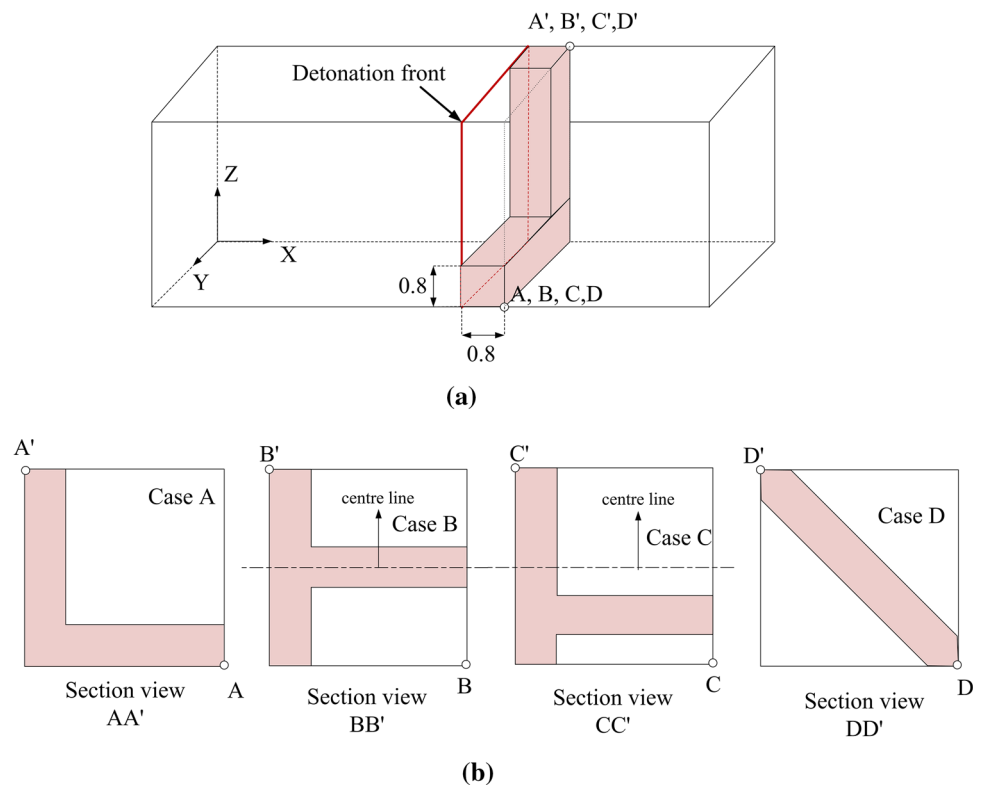
4 Results and discussions

4.1 Rectangular in phase to spinning detonation (Case A)

The structure of initial perturbation in case A is introduced in Fig. 2. By applying this perturbation, a rectangular in-phase structure emerged at the early stage of computation. The typical shock wave structures are observed in each boundary wall. The triple lines appear at the boundary between the Mach stem and the incident shock wave. In Fig. 3a, we can observe the appearance of a system of two orthogonal triple lines, a spherical Mach stem and an incident shock. The two orthogonal triple lines move along the front parallel to Y direction and Z direction, and the incident shock collision with the two neighbouring walls produces a new spherical Mach stem. The similar waves are observed in each two neighbouring walls. The two Mach stems propagate along the front diagonal and in opposite directions as shown in Fig. 3b. The triple lines are divided into two subsections with position differences caused by the collision of the triple lines and the spherical Mach stem (see Fig. 3c). The Mach stem and the incident shock interchange their roles via this collision as the detonation propagates. The triple lines move to another two neighbouring walls in phase as shown in Fig. 3d, and the similar evolution of front is observed as above. The cycle time of rectangular in-phase mode is approximately 2.5 times $t_{\text{reference}}$.

The localized explosions and shock–flame interactions lead to detonation front instabilities which strengthen flow instabilities. The symmetry of the two orthogonal triple lines breaks down, and the triple lines reach each opposition of original wall at the different time (out of phase) (see Fig. 4a–c). In addition, the corner spherical Mach stem moves to the centre of the wall. Due to the sustained energy, the detonation forms a stable propagating mechanism, which is a spinning detonation. The formation of a self-sustained spinning structure is observed at $t = 40.8333$. The detonation front is mainly composed of three Mach stems, one incident shock and various small irregular shape Mach reflections (see Fig. 4e). Each collision of the transverse shock and vertical triple line with the sidewall produces high-pressure area or forms a strong explosion centre, which changes the rotating direction of transverse detonation and sustains the detonation propagation (see Fig. 4d and f).

Figures 5 and 6 show the evolution of the spinning front and pressure contours during one period. The complex Mach reflection and transverse detonation are present with two transverse waves perpendicular to each other. The unburned gas pocket and the explosion center, which accelerates the growth of the flow instabilities in spinning detonation, produce the irregular detonation front and variable phase difference. However, the main characteristics of spinning detonation are still present, and its rotating direction is constant. As the sustained spinning detonation develops, it appears that most of the phase difference is close to 90°. Subsequently, the detonation front presents a periodic structure evolution identical to "Fig. 3" of Tsuboi et al. [20]. It is also found
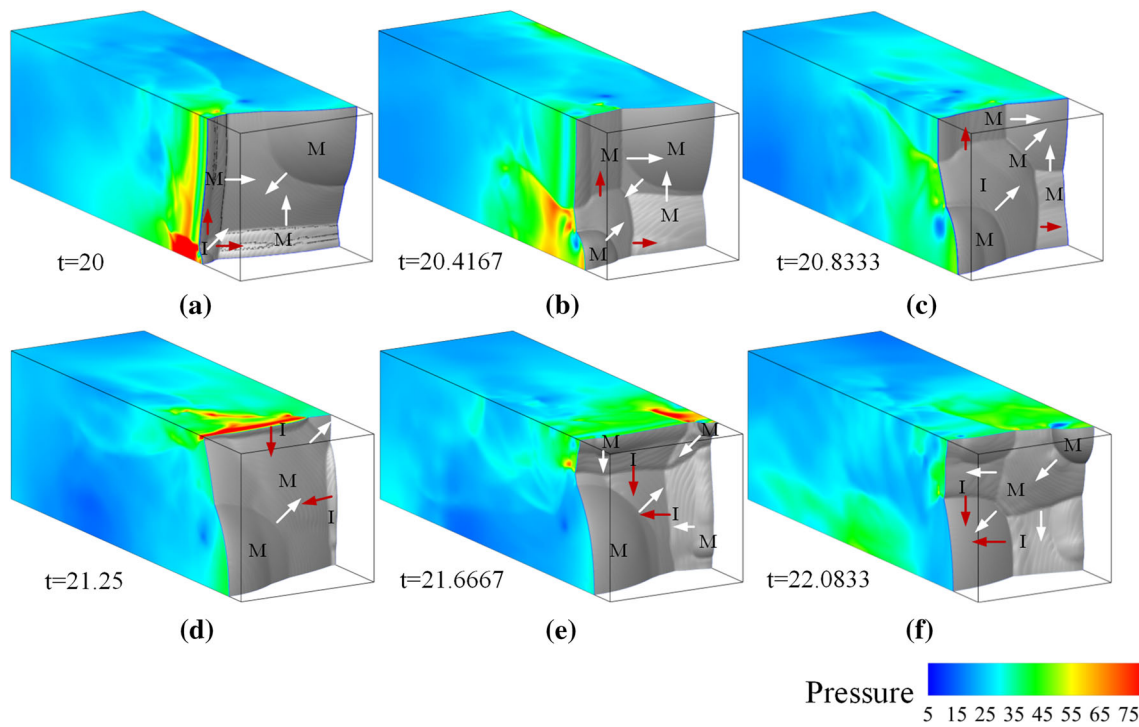
Fig. 3 Evolution of the rectangular in phase structure during one period. The *gray* isosurface denotes the detonation front and the wall surface represents pressure contours
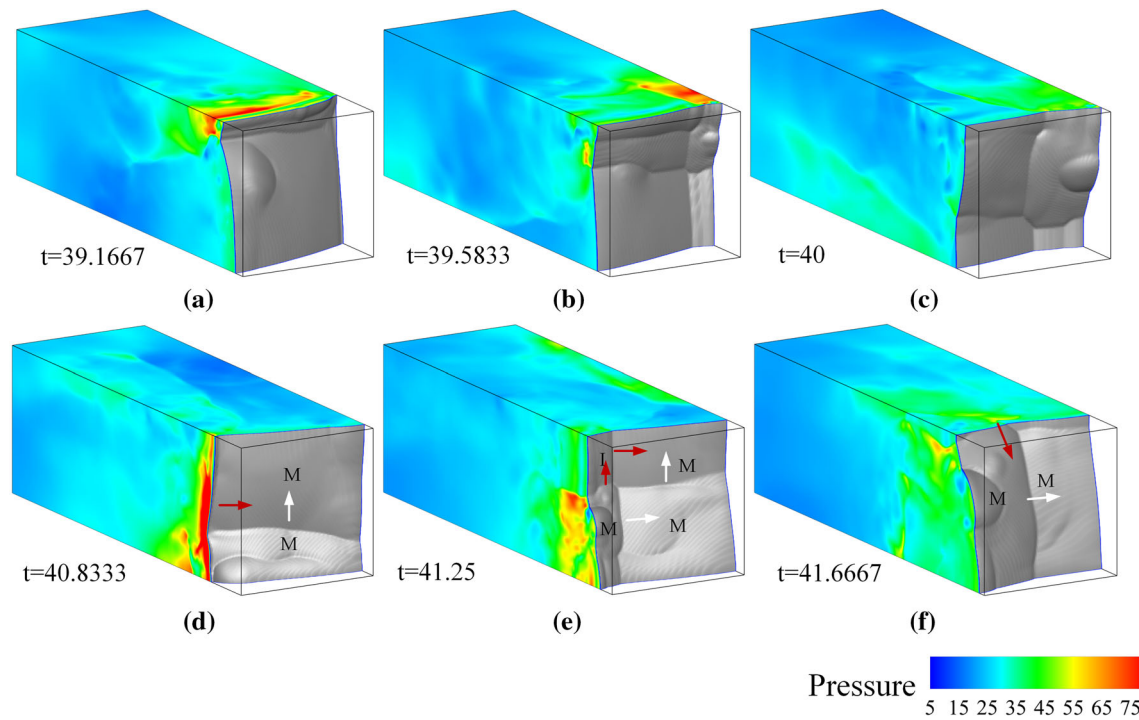
Fig. 4 Evolution of the detonation fronts (from *rectangular* in phase to spinning structure)
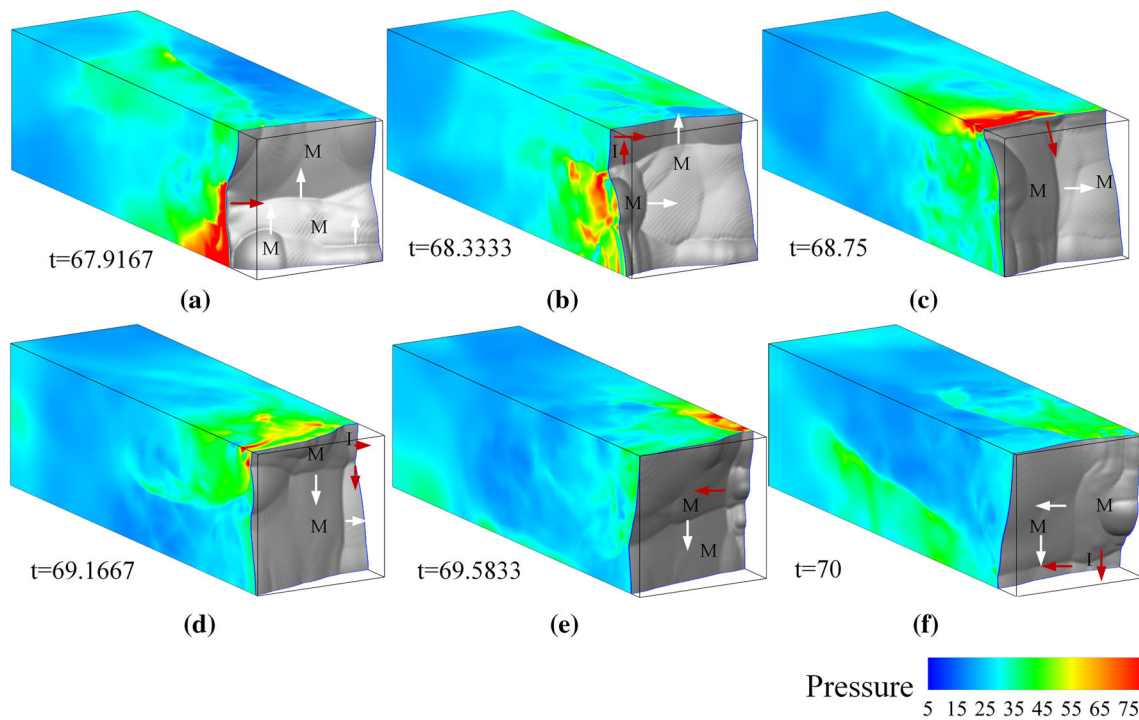
Fig. 5 Spinning detonation front at various times. The *gray* isosurface denotes the detonation front and the wall surface represents pressure contours
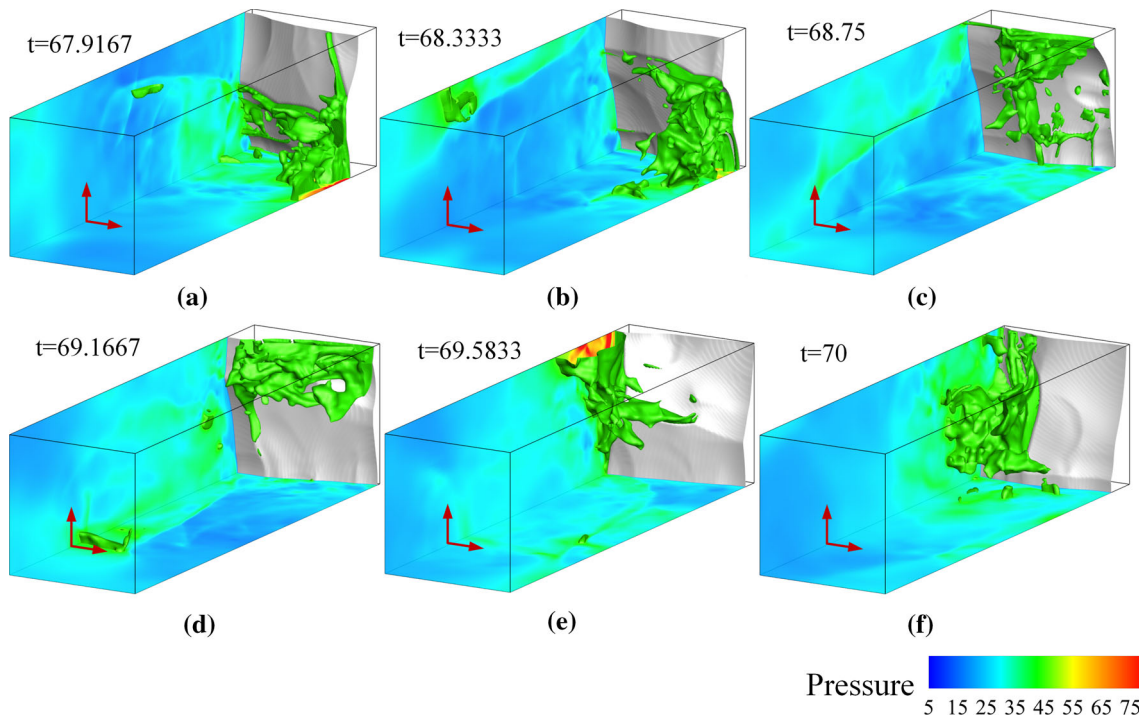
Fig. 6 Rear view of Fig. 5. The *green* space isosurface in pressure is the pressure of 45

that the reflected shock extended backwards into the burned gas in Fig. 5f and it agrees well with results in both experimentally by Edwards et al. [28] and numerically by Tsuboi et al. [20]. However, a multitude of triple line and smaller Mach stems have emerged on the front, which caused by the stronger flow instabilities of this case. Among them, the main triple lines and Mach stems are stronger than the rest. We can see from Fig. 6 that the spinning front happens to take on a counterclockwise rotation, and the explosion areas are also observed away from the leading front.

Fig. 7 Maximum pressure history on the tube walls at various locations. The direction is from *left* to *right*
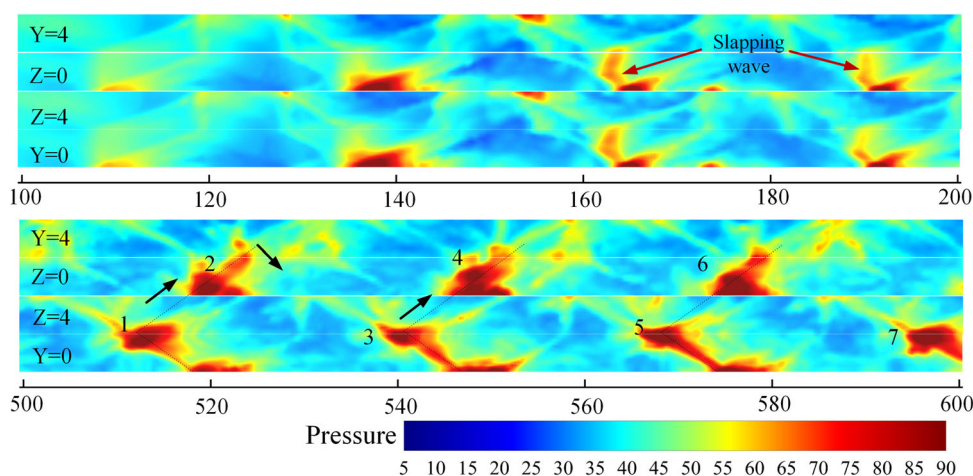

Figure 7 shows the maximum pressure history on the side walls at the various stages of detonation evolution. Similar patterns are formed on the two adjacent walls ($Z = 0$ and $Y = 0$, $Z = 4$ and $Y = 4$) at the stage of rectangular in-phase mode. The slapping waves in the transverse direction appear in Fig. 7a. This is indeed observed from Fig. 3, and it was confirmed by the experiment of Hanana et al. [5]. The transition from rectangular in phase to spinning detonation happens at around $X = 400$. Figure 7b displays the spinning detonation pattern, where the track is the recording of the maximum pressure on the side walls. The track angle of the spinning detonation is around 40°. A single-headed spinning detonation pattern, which is observed experimentally and numerically in a square channel, has the single helical trajectory of the spin head [6,20]. Comparing the present simulation with those in [20], the hydrodynamic instability is stronger than that of [20], which is observed from Fig. 5. In addition, the present one-step reaction exists stronger intrinsic physical instability as compared with a detailed chemical reaction model [26]; as a consequence, the detonation front is more unstable and distorted. Thus, the distinct single helical trajectory is not observed in the present simulation. However, the similar features are present with these tracks in a helical line. The maximum pressure tracks are in a helical line but with a tail which is due to track of the reflection of the triple line collisions (see Fig. 7b). In addition, it can be seen that the similar patterns are formed after $X = 455$ and, therefore, the spinning detonation is sustained and stable.
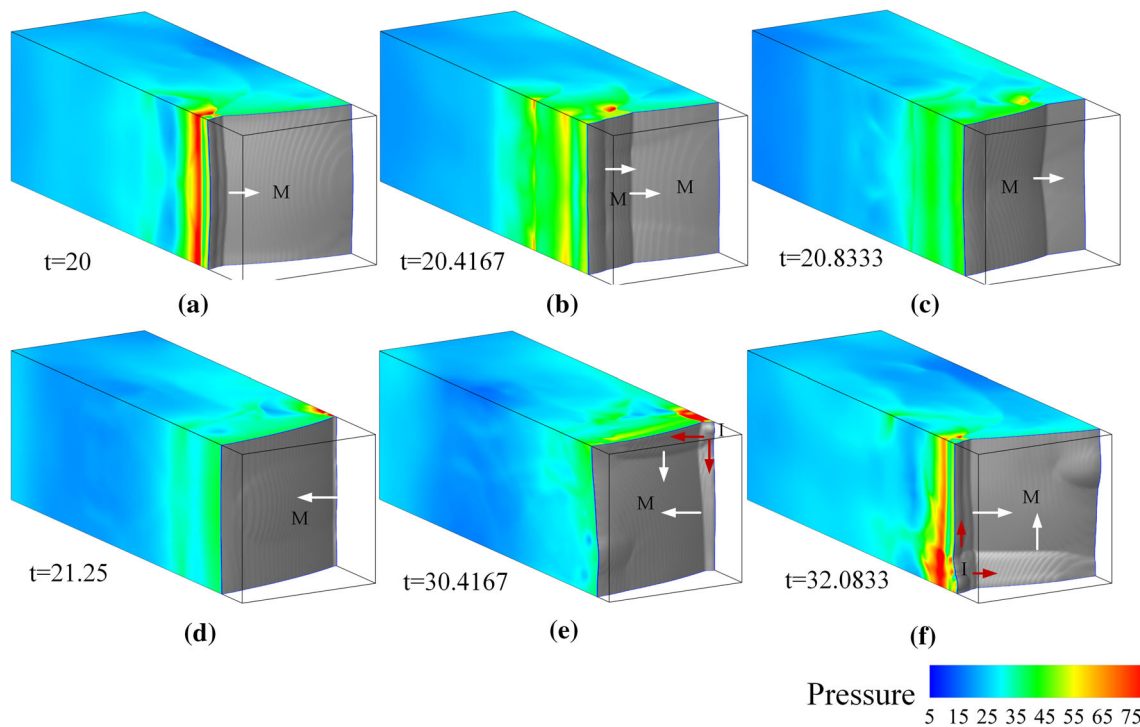
4.2 Rectangular out of phase to spinning detonation (Case B)

A rectangular out of phase perturbation is applied to accelerate the growth of the flow instabilities (see Fig. 2b). This perturbation leads to the formation of a rectangular out of phase structure, which is different from the rectangular out of phase structure in large rectangular duct in [5]. The median pressure increasing pocket spreads to both sides and decay rapidly. Thus, the lateral pressure pockets dominate the front structure and produce a pair of triple lines parallel to Z direction in the front view of Fig. 8a–d. The triple lines propagate along the front perpendicular Z direction. When the triple lines reach the wall, the direction of propagation changes to be opposite due to the collision between a triple line and a wall. By the time $t = 30.4167$, a system of the two orthogonal triple lines and a Mach stem is formed, similarly to case A. However, the location and strength of the Mach stem are different from case A. Subsequently, the similar evolution of detonation is observed (see Fig. 8f). Finally, the detonation becomes spinning structure at $t = 37.9167$, which is less than the time of case A. A similar spinning structure evolution with multitudes of triple line and various small irregular shapes of Mach stem is also observed (not shown here). It is interesting to observe that typical feature of spinning (three Mach stems and one incident shock separating by the triple lines) is not apparent, occasionally.

Figure 9 shows the maximum pressure history on the side walls at the various stages of detonation evolution. Due to the width of the pockets of pressure increase, two transverse waves emerge at $Y = 4$ in Fig. 9a. When a transverse wave approaches the wall of $Y = 0$, the collision of transverse wave with the wall produces a large-area track at $Y = 0$. This kind of pattern is not changed until the front transformed into a rectangular in-phase structure. The transition to spinning detonation happens at around $X = 375$. Figure 9b displays the spinning detonation pattern which is almost same with case A but with a phase difference of 180°. The track angle of the spinning detonation is around 38°. The spinning front happens to take on a counterclockwise rotation, and propagates with a certain frequency that could be changeable within two cycles.

Fig. 8 Evolution of the detonation structure. The *gray* isosurface denotes the detonation front and the wall surface represents pressure contours

Fig. 9 Maximum pressure history on the tube wall at various locations. The direction is from *left* to *right*
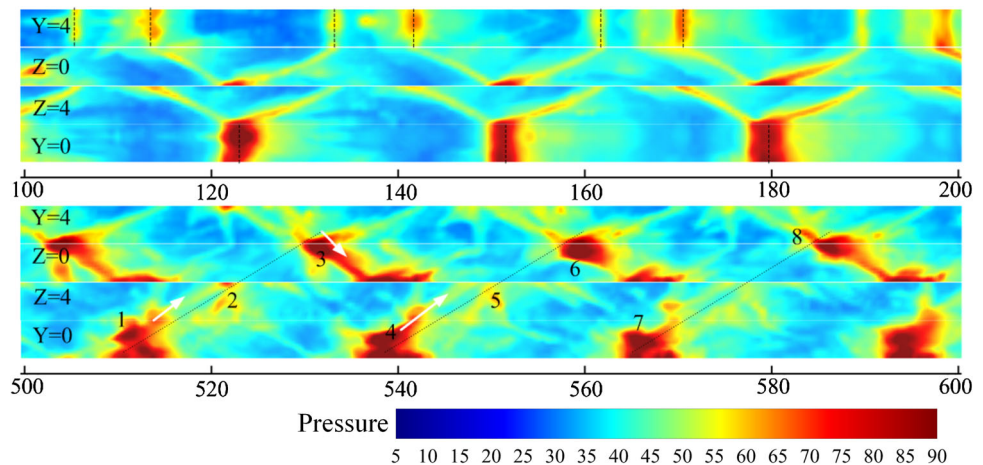
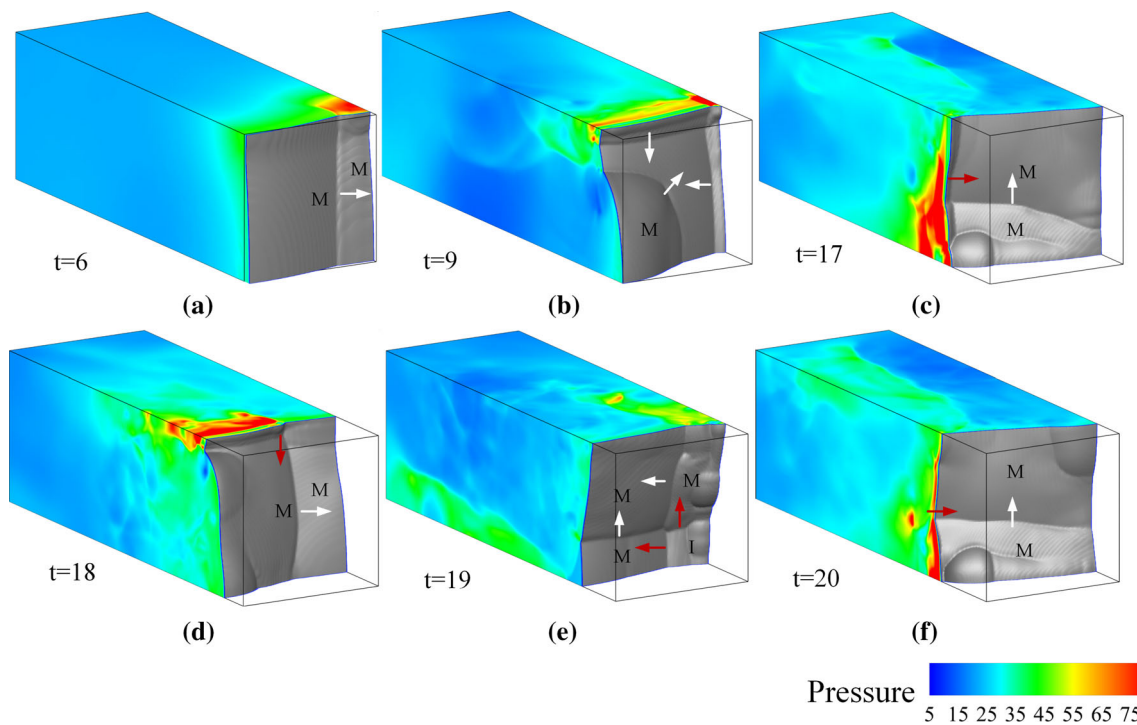### 4.3 Rectangular partial out of phase to spinning detonation (Case C)

A rectangular partial out of phase perturbation is applied to accelerate the growth of the flow instabilities (see Case C in Fig. 2b). This perturbation leads to the formation of rectangular out of phase structure, but a pair of triple lines is not parallel to Z direction due to this asymmetrical perturbation (see Fig. 10a). The front structure transforms into rectangular in phase at $t = 9$ as shown in Fig. 10b. Finally, the detonation evolves into spinning detonation at $t = 17$ (see Fig. 10c). It is possible that due to the asymmetry of initial perturbation, the spinning detonation emerges in the shortest time compared to other three cases. Similar spinning detonation structure is

also present in Fig. 10c–f, and the reflected shock extends backwards into the burned gas (see Fig. 10e, f). The spinning front also takes on a counterclockwise rotation.

Figure 11 shows the maximum pressure history of spinning detonation. The spinning detonation pattern is similar with case B. The transition to spinning detonation happens at around $X = 200$ and the track angle of the spinning detonation is also around $38°$.

4.4 Diagonal to spinning detonation (Case D)

The structure of initial perturbation in case D is introduced in Fig. 2. Figure 12 shows a detonation wave front and pressure contours at the early stage of the computation. The collisions

Fig. 10 Evolution from the *rectangular* partial out of phase to the spinning structure. The *gray* isosurface denotes the detonation front and the wall surface represents pressure contours

Fig. 11 Maximum pressure history of spinning detonation on the tube wall. The direction is from *left* to *right*
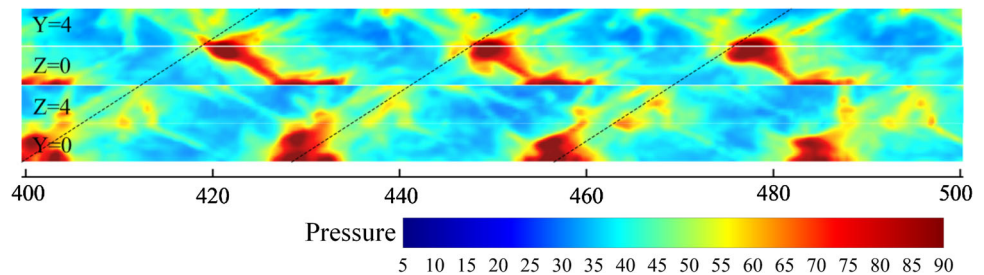

of the triple lines and explosions occur at a corner as shown in Fig. 12b, and the high-pressure shock front is generated. The shock wave reaches a corner, and a Mach stem is produced due to the reflected shock. The shock waves and Mach stems propagate diagonally and in the same direction. When a pair of shock front collides with each other at the diagonal line, a pair of new Mach stems is produced as shown in Fig. 12d. This new Mach stem propagates along diagonal directions. When the two Mach stems meet as shown in Fig. 12f, the new stronger Mach stem dominates the direction of propagating. The detonation front is composed of two pairs of Mach stems and one pair of incident shock waves as well as reflected shock. The cycle time of diagonal mode is approximately 9.1667 times $t_{\text{reference}}$ and a partial change in the detonation front occurs later.

Figure 13 shows the rear view of the detonation front evolution, and the green space isosurfaces indicate the high-pressure areas at 45. It can also be seen from Fig. 13 that

there is a quasi-symmetrical structure within the diagonal structure. The quasi-symmetry breaks down, and the collisions of the triple lines drift off the diagonal lines soon afterwards. The disturbance is intensified by the irregular high-pressure area, which accounts for the disappearance of quasi-symmetrical.

Figure 14 shows the maximum pressure history on the side walls at the various stages of detonation evolution. Similar patterns are formed on the two adjacent walls ($Z = 0$ and $Y = 0, Z = 4$ and $Y = 4$) at the stage of diagonal detonation. This was indeed confirmed by the experiment of Hanana et al. [5]. This pattern breaks down when the detonation front propagates at around $X = 400$. The diagonal detonation transitions to spinning detonation at around $X = 470$. The spinning detonation pattern is shown in Fig. 14b, where the track is the recording of the maximum pressure on the side walls. The track angle of the spinning detonation is around $40°$. When the transverse detonation and triple line collide
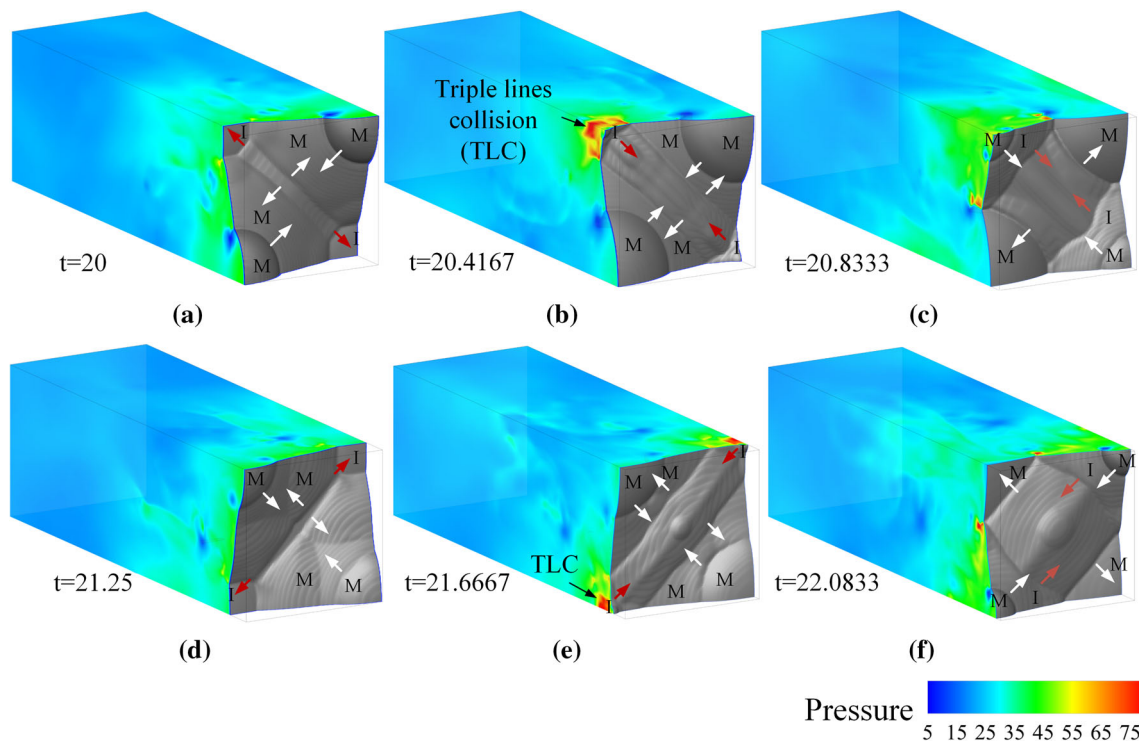
Fig. 12 Evolution of the *diagonal* detonation front at the early stage of the computation. The *gray* isosurface denotes the detonation front and the wall surface represents pressure contours

with $Z = 4$ and $Y = 0$, a strong explosion appears near the two side walls leading to a track labeled by 1 due to high pressure. The transverse detonation changes the rotating direction upward. As it propagates, the next collision (track 2) happens at the walls of $Y = 4$ and $Z = 0$. This collision will change the rotating direction toward the bottom. It is clearly seen that the maximum pressures are less than those in case A, B and C.

4.5 Transverse waves dynamics

The detonation front structures depend on the types of initial disturbance, which will produce flow instabilities in the leading shock front. Flow instabilities strengthen the detonation front instabilities which, in turn, result in the irregularity of the front structure. Hydrodynamic instability analysis of detonation waves shows that q, E_A and f are the key detonation parameters which act as the detonation flow dynamics. The present parameters have been used in numerous previous numerical studies [14,25]. However, the results of the 2-D and 3-D simulations are inconsistent. It is clear that the detonation structure is quite regular in two-dimensional simulation [14] and totally differs from the irregular structure of detonation in [25]. As mentioned above, it is found that the transverse shocks play an important role in the detonation propagation. Based on the results of simulations, we try to clarify the transverse waves dynamics in the 3-D deto-

nation propagations and its role in the detonation structure transformations.

Figure 15 displays the detailed structures of the head of the detonation with transverse waves on the walls corresponding to Fig. 13. There is a one-to-one correspondence between the triple points (A–H and 1–5) in Fig. 15 and the intersection points (A–H and 1–5) of the high-pressure areas with walls in Fig. 13. The formations of transverse waves are caused by the collisions of triple lines with walls or triple lines with triple lines as well as the explosion behind the fronts. The diagonal structures are observed with the triple line formation on a plane normal to the diagonals. The transverse wave structures on the four sidewalls are almost same but with phase difference of 180° between walls $Z = 0$, $Y = 0$ and $Z = 4$, $Y = 4$ at $t = 20$ and 25.8333. The primary triple point A joints the short transverse wave and the leading shock which is made of the incident shock and Mach stem. B is the second triple point which has its own transverse wave. It is seen from Fig. 16 that the interaction of a vortex with the Mach stem or incident shock causes significant curvature and produces a secondary triple point, which divides the shock into various segments with different strengths and wave angles. Due to the high flow instabilities, ignition of the unburned gas pocket through the high temperature and turbulent mixing, and partial hot spots, the regularity of the transverse wave disappears gradually (see $t = 45.8333$ in Fig. 15), and the diagonal mode evolves into the spinning mode at $t = 49.1667$. The disappearance of
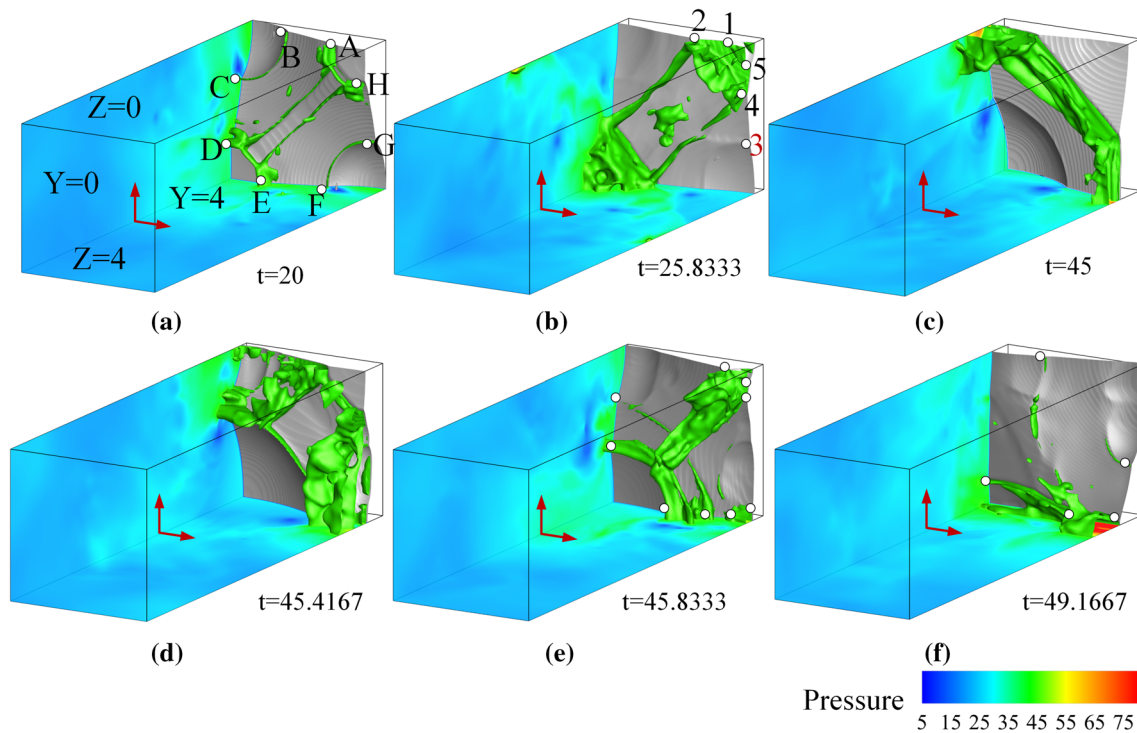
Fig. 13 *Rear view* of detonation front evolutions (from *diagonal* to spinning structure). The *green* space isosurface is the pressure of 45. (*Up*, *left*, *bottom* and *right* wall are $Z = 0$, $Y = 0$, $Z = 4$ and $Y = 4$ plane, respectively)

Fig. 14 Maximum pressure history on the tube wall at various locations. The direction is from *left* to *right*
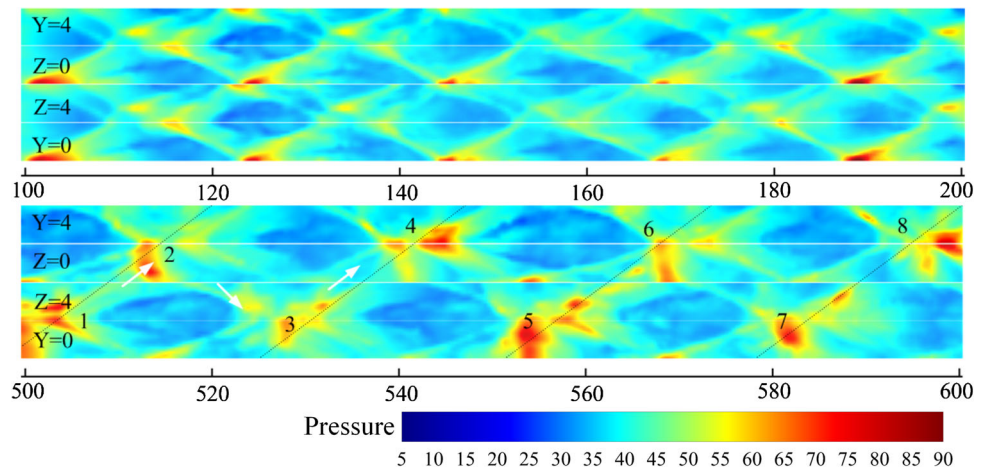

transverse waves is observed on the walls $Z = 0$ and $Y = 0$ at $t = 49.1667$, whereas the intricate transverse waves are present on the walls $Z = 4$ and $Y = 4$.

The complex sub-structures of transverse wave of spinning detonation head in the case D are present in Fig. 17. A long unstationary transverse wave travels regularly upwards and downwards at various times. The transverse wave of spinning detonation is characterized by the reflected shock extended backwards into the burned gas (see RS in Fig. 17) and the constant appearance and disappearance of transverse waves on the different walls. The generation of reflected shock is due to the collision of two shocks with different wave

angles. The constant appearance and disappearance of transverse waves were also observed in the high irregular structure experimentally by [8]. The reason is that the local explosion due to triple line collisions and unburnt gas pockets affects the transverse wave formation at the walls far from the spin head. However, the 3-D transverse waves of spinning detonation always emerge in all snapshots. This is indeed confirmed by the transverse wave dynamics on the face of $Y = 2$ (see Fig. 18). The spinning detonations have the strong transverse detonation rotating along the walls and the transverse waves will disappear at the interspace between the helical line and the walls due to the spin head deviated from these walls.
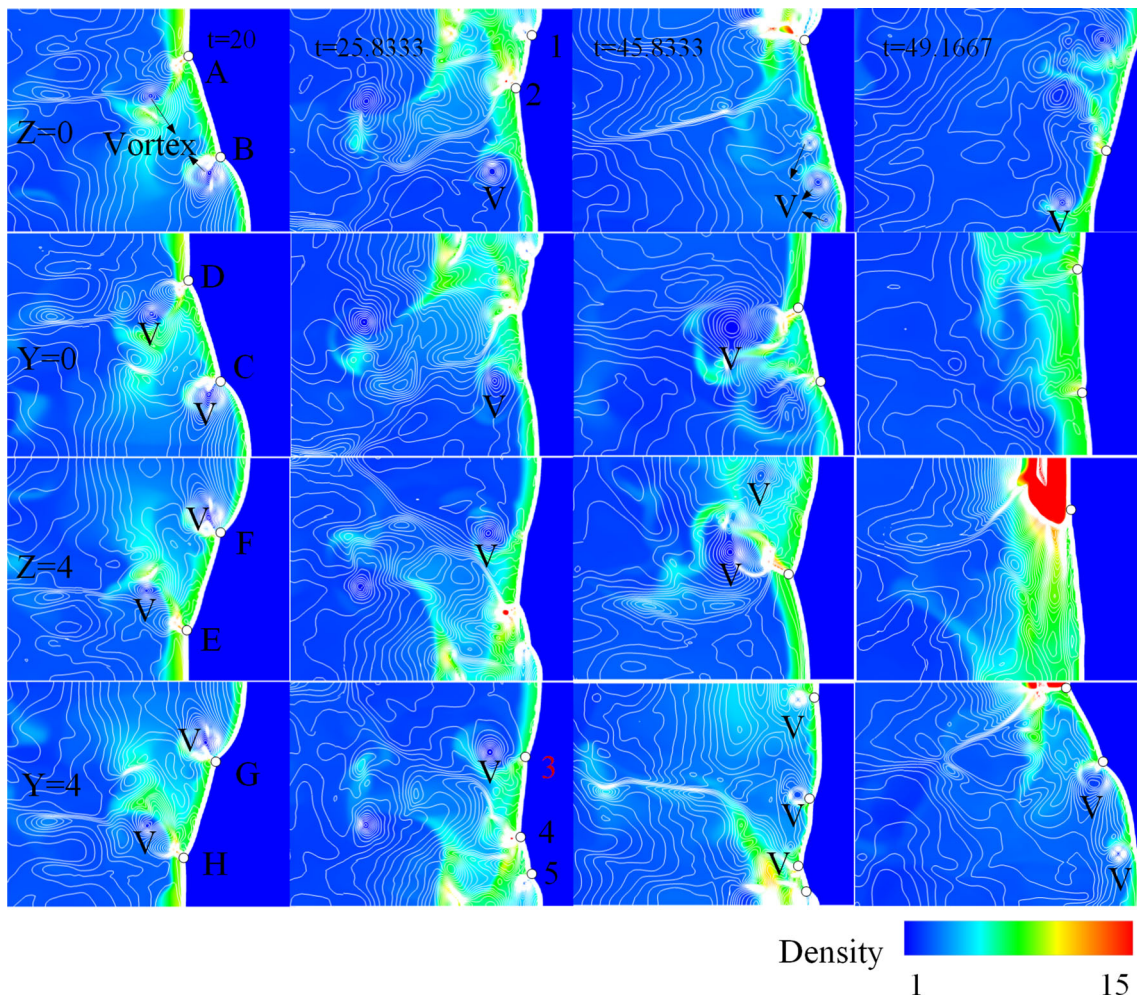
Fig. 15 Detailed structure of the head of the detonation with transverse waves on the walls. The *labels* refer to Fig. 13. *V* stands for Vortex. The *color* and *white line* represent density and pressure contours, respectively (Case D)
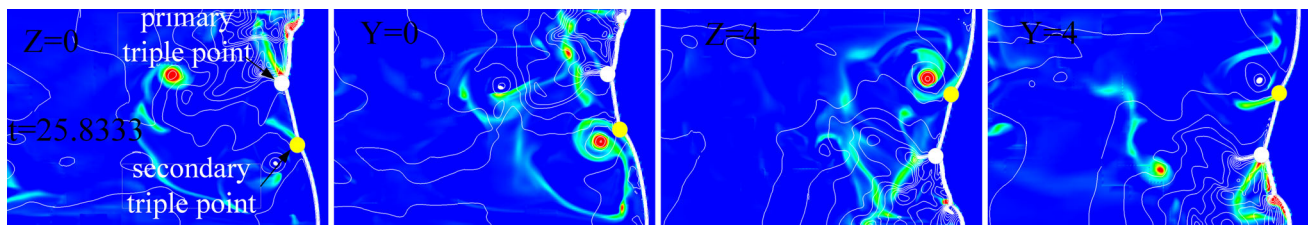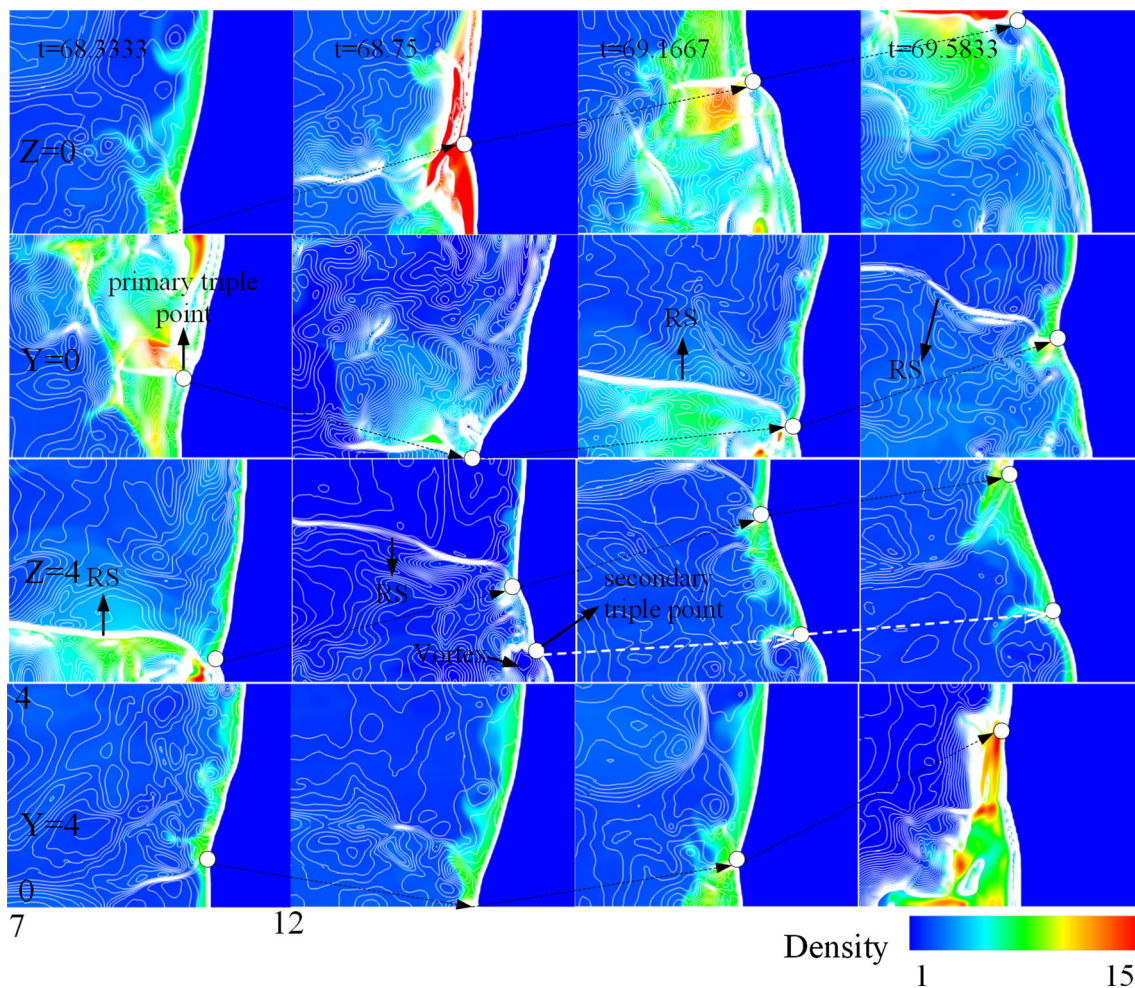

Fig. 16 Detailed structure of transverse waves with vortex and shock. The *color* and *white line* represent vorticity and pressure contours, respectively (Case D)

The similar complex sub-structures of transverse wave of spinning detonation are observed in other three cases.

A typical sub-structure in the diagonal detonation structure is observed in Fig. 18 (up four snapshots), which agrees fairly well with the 2-D numerical results by Ji et al. [25]. The overall structure of the spin head is similar to "Fig. 7" in the simulation of Tsuboi et al. [20]. However, the detailed sub-structures of the spinning detonation are different, and no secondary triple point was observed in their results. This could be due to the fact that the more stable reaction model was employed in the [20], which is consistent with the results reported by Mahmoudi et al. [14]. It is seen from Fig. 18 that the Mach stems and incident shock interchange their roles via the collision of triple lines and walls. The similar structures of transverse wave are also observed in other three cases.

Figure 19 shows the transverse waves in space and in time on the stage of transition to spinning. Due to the flow instability increase, a complex transverse wave structure is formed
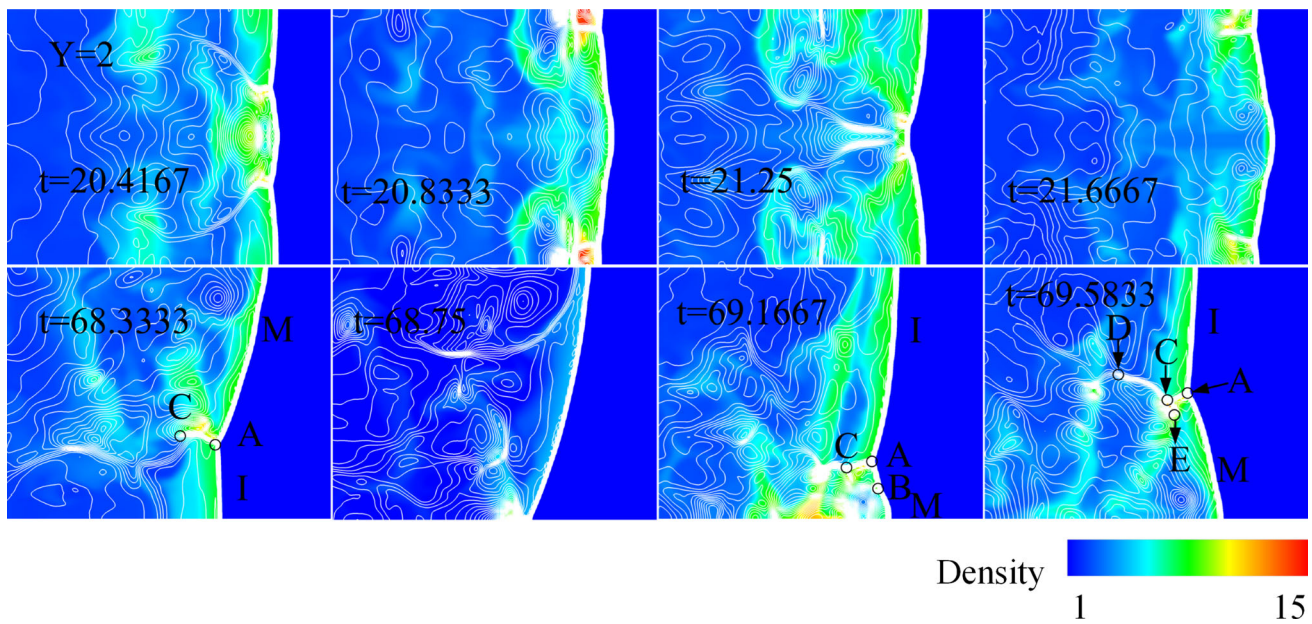
Fig. 17 Detailed structure of the head of the spinning detonation with transverse waves on the walls at successive snapshots. *RS* stands for reflected shock. The *color* and *white line* represent density and pressure contours, respectively (Case D)

at $t = 45$, in which three transverse waves are present. The vortex between B and C point decays, in turn the C point finally diminishes, and the new vortex appears in the vicinity of AD (see the second snapshot of Fig. 19). The occurrence of localized explosions (the vicinity of AD in second snapshot of Fig. 19) turns the transverse wave's directions and leads to KH instability, which creates vortices between A and B point. Due to the localized explosions, transverse wave A is strongly overdriven. The transmitted wave propagates into the burned gas left behind transverse wave A and, therefore, gains little chemical energy release to sustain itself. As the vortex in the vicinity of BE decays, eventually the only one primary transverse wave A dominates the front as shown in the fourth plot of Fig. 19. As a consequence, the spinning detonation structure is formed. The occurrence of localized explosions and unburned gas pocket accelerates the growth of the flow instabilities. However, the analogous structure of the fourth or fifth snapshot of Fig. 19 is the most stable transverse structure in all cases.

As mentioned above, it is found that the vortical structures exist in the detonation front in all the cases. It is possible that the generations of large vortices behind the front play an important role in the transformation of the transverse waves and the leading shock waves which lead to the formation of the spinning detonation. Additionally, the temporal and spatial variation of transverse waves leads to the front instability.

Transverse wave structure of spinning detonation is shown at $t = 68.3333$ of Fig. 19. Due to the existence vortex, the structures of spinning front are intricate with the schematic structure of the spin as proposed in [6] and 3-D simulation by Tsuboi et al. [20]. However, it is clearly seen that the triple point configuration mainly consists of a Mach stem, incident shocks and transverse waves. The transverse wave strength S (p_2/p_1) plays an important role in detonation propagation [20]. To evaluate its value, we define the pressure at both up and bottom sides of transverse wave as p_1 and p_2 located next to the side of incident shock and Mach stem, respectively. We extract 100 points along both up and bottom sides of

Fig. 18 Detailed structure of the head of the detonation on the face $Y = 2$. The *color* and *white line* represent density and pressure contours, respectively. *A* primary triple point, *B* secondary triple point, *AM* Mach stem, *AI* primary incident shock, *ACD* primary transverse wave, *AC*, *CD* and *CE* reflected shock
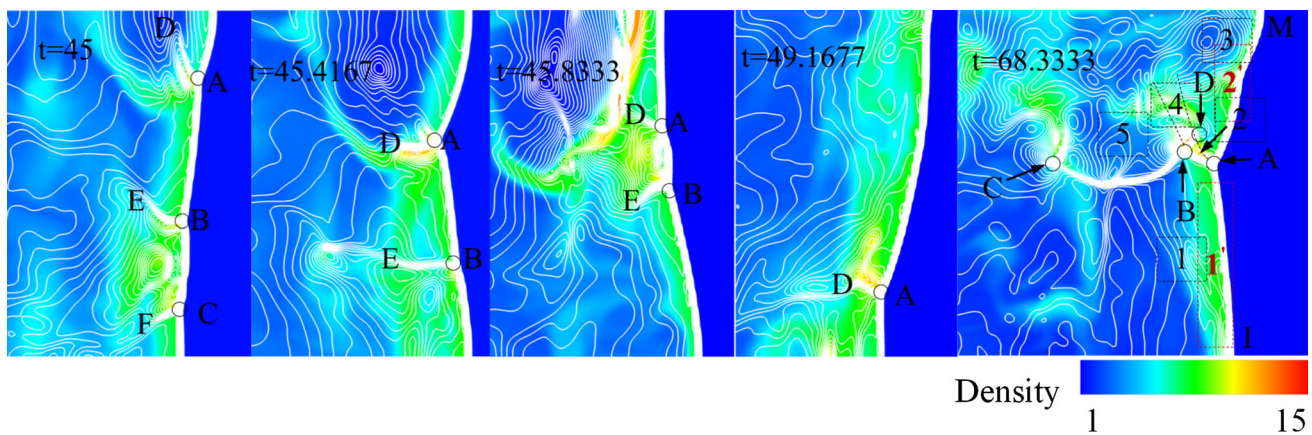

Fig. 19 Transverse wave in space and in time of Case D

transverse wave, separately. In this case, the averaged values of 100 points are adopted as p_1 and p_2 separately, because it is difficult to define the exact value of p_1 and p_2.

The maximal pressure behind the detonation head and transverse wave strength during different stages is plotted in Fig. 20. At the stage of the diagonal structure, the transverse wave strength is larger than 0.95, and the average value of the maximal pressure is around 82. In the process of the transition to spinning structure, the average values of the maximal pressure increase. The transverse wave strength suffers large fluctuations in time and space. As mentioned in Fig. 19, due to the chaotic distribution of transverse waves, it is difficult to evaluate its strength. It is clear that the transverse wave strength of spinning detonation is fluctuant compared to the

stage of diagonal structure. From Figs. 18 and 20, we can see that the transverse wave strength becomes larger after the collision of the triple lines with the side wall. The detonation strengthens (the average maximal pressure is around 125) and the front suffers the large pressure oscillations. The transmitted and reflected wave propagates into the burned gas left behind the front and, therefore, gains chemical energy release to sustain spinning detonation. Thus, the spinning detonation is self-stained and fairly stable. The periodic oscillations of the leading shock and transverse wave dynamics are involved in the 3-D detonation structure transformations.

A comparison of detonation parameters among the four cases is given in Table 1. The track angle is mainly related to the specific heat ratio [20]. The track angles of the present
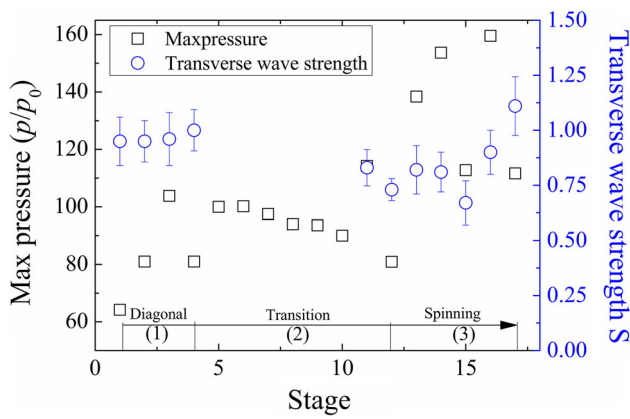
Fig. 20 Evolution of the max pressure and transverse wave strength behind the head of the detonation front on the face of $Y = 2$ during the whole period

simulation are around 38–40, which are measured from the pressure contour on the wall. The present results are reasonably consistent with the experimental and numerical studies [20,26], and [28]. The different initial disturbances lead to different evolution of the detonation structure and, finally, all the cases transform into the self-sustained spinning detonations. The case C takes the shortest time and distance to a stable spinning detonation. The maximal pressures behind the spin head are 160–225.2 p_0 and such high pressures are to be avoided in practical systems in the safety problem. On the contrary, such high pressures are beneficial for the performance of the micro-pulse detonation engine [29]. The transverse waves strength [2,20] in the case A, B and C are around 1.1, which is greater than that of case D. It is interesting to mention that the disturbance is totally asymmetric in case C. It is possible that the asymmetric disturbance leads to the strong flow instabilities which could be the main driving force of detonation transformation into the spinning detonation.

4.6 Effects of channel width on spinning detonation transformation

To understand the effects of channel width on three dimensional structure of the spinning detonation, the computational domain in cross section is two times as above with dimen-

sions of $[0, 24] \times [0, 8] \times [0, 8]$. The initial conditions and boundary conditions are same as the above mentioned in 3.2. Figure 21 shows the instantaneous pressure space isosurfaces and contours of spinning detonation within the double times channel width. A spinning structure evolution with multitudes of triple line and various small irregular shapes of Mach stem is also observed as the numerical results in the half cross section. The spinning detonation formations are independent of any initial perturbations.

The complex sub-structures of transverse wave of spin head are present in Fig. 22. Due to an analogous structure of each other, not all the details about other cases are discussed. The transverse wave of spinning detonation has similar features but with absence of reflected shock extended backwards into the burned gas. Due to the localized explosions, transverse wave is strongly overdriven and the vortex emerges.

In summary, the detonations will transform into the spinning detonation in the narrow square tubes with the approximate channel widths 0.8 and 1.6 mm, and the spinning detonation is the most stable propagating mode and its formation is independent of the initial perturbations. However, the dependence of the critical diameter on the spinning formation should be studied in the future.
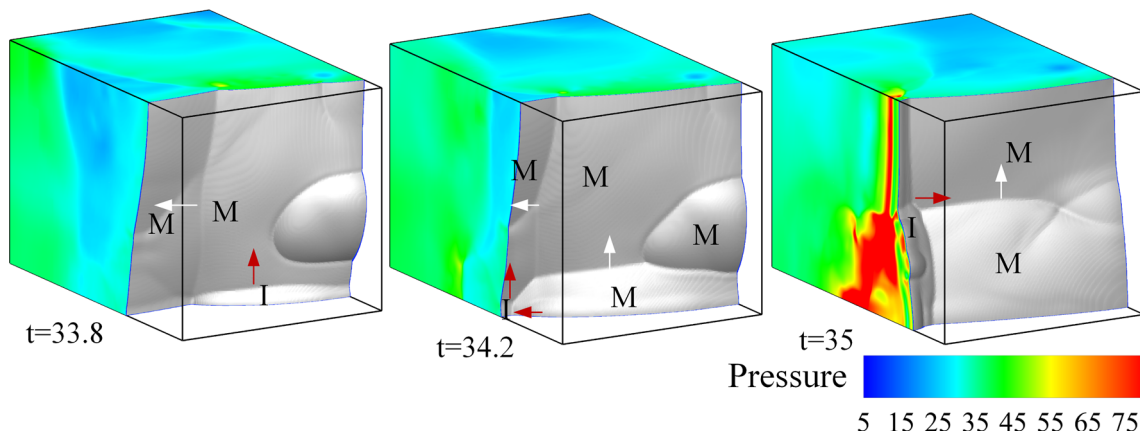
5 Concluding remarks

Three-dimensional simulations of the structures of detonation in two narrow square tubes (around 0.8 and 1.6 mm in width) have been performed. The high-resolution simulations were conducted with a parallel AMR algorithm using high-order MUSCL-type TVD scheme and new CSAMR data structure. The four different perturbations applied in the initial ZND profiles lead to the different types of detonation structure (diagonal, rectangular in phase, rectangular out of phase and rectangular partial out of phase) at early stage, eventually all the detonations evolve into self-sustained spinning detonation. The present simulation showed the detailed transformation processes from the diagonal and rectangular into spinning structure.

Detailed structures for the diagonal, rectangular (in phase, out of phase, partial out of phase) and spinning have been

Table 1 Comparison of the track angle, time and location of transition to spinning structure, maximal pressure behind the spin head and transverse wave strength

Case	Track angle (o)	Spinning detonation transition time ($t_{reference}$)	Transition location ($l_{reference}$)	Maximal pressure behind the spin head (p_0)	The average value of transverse wave strength behind the spin head $\bar{S}_{spin}$
A	40	40.8333	400	225.2	1.1
B	38	37.9167	375	186	1.15
C	38	17	200	221.6	1.08
D	40	49.1667	470	160	0.8

Fig. 21 Instantaneous pressure space isosurfaces and contours of spinning detonation for double times width domain. The *gray* isosurface denotes the detonation front and the wall surface represents pressure contours
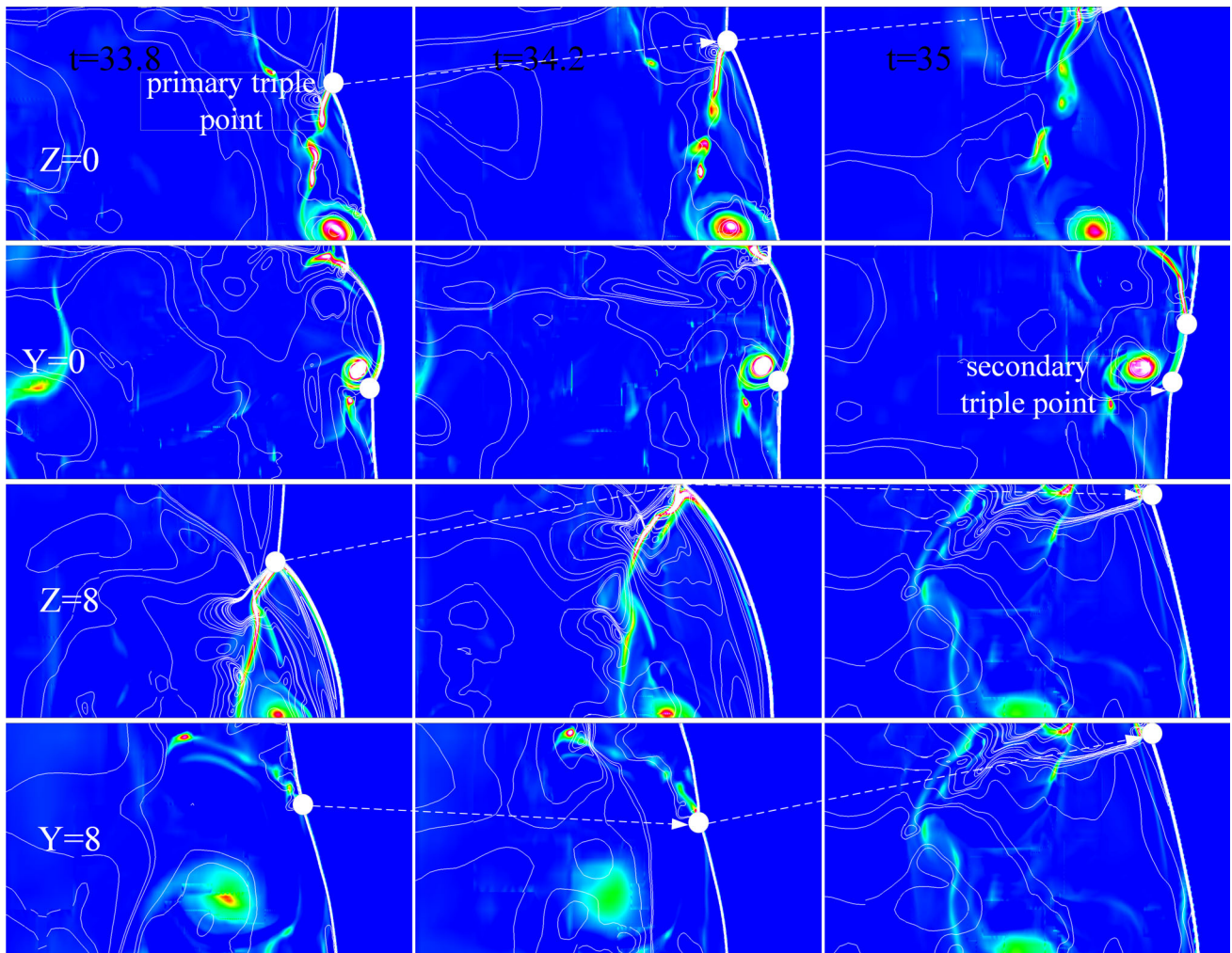
Fig. 22 Detailed structure of the head of the spinning detonation with transverse waves on the walls at successive snapshots. The *color* and *white line* represent vorticity and pressure contours, respectively

presented. Those results are in good qualitative agreement with available the experimental and numerical studies.

The spinning detonation is the most stable propagating mode and its formation is independent of the initial perturbations and the narrow channel widths. The effects of critical diameter should be also estimated.

The "rectangular partial out of phase" perturbation leads to a stable spinning detonation much faster than the rest. The transverse wave strength behind the spin head in case D is less than the rest cases. The maximal pressures behind the spin head are 160–225.2 p_0. Thus, the quick transition into a spinning detonation is the most effective way to attain stable detonation in a small tube and improve the performance of the pulse detonation engine.

The asymmetric disturbance leads to the strong flow instability which is the main drive of detonation transformation into the spinning detonation. The flow instability strengthened the detonation instability. The periodic oscillations of the leading shock and transverse waves dynamics are involved in the detonation instability. The transverse waves always emerge in the 3-D spinning detonation and the disappearance of transverse waves on the walls is due to the spin head deviation from these walls during the rotation of spinning detonation. In all cases, the transverse wave dynamics and periodic oscillation of front play an important role in the detonation structure transformations.

Finally, the present simulations provide a complementary understanding of the detonation dynamics and propagation in a narrow square tube and elucidate the drive of the detonation structures transformations.

References

1. Fickett, W., Davis, W.C.: Detonation. University of California Press, Berkeley (1979)
2. Strehlow, R.A., Biller, J.R.: On the strength of transverse waves in gaseous detonations. Combust. Flame **13**, 577–582 (1969)
3. Strehlow, R.A.: Multi-dimensional detonation wave structure. Astronaut. Acta **15**(5), 345–357 (1970)
4. Takai, R., Yoneda, K., Hikita, T.: Study of detonation wave structure. Proc. Combust. Inst. **15**, 69–78 (1975)
5. Hanana, M., Lefebvre, M.H., Van Tiggelen, P.J.: Pressure profiles in detonation cells with rectangular and diagonal structures. Shock Waves **11**, 77–88 (2001)
6. Lee, J.H.S.: The Detonation Phenomena. Cambridge University Press, Cambridge (2008)
7. Lee, J.H.S., Soloukhin, R., Oppenheim, A.K.: Current views on gaseous detonation. Acta Astronaut **14**, 565–584 (1969)
8. Mach, P.: Bifurcating Mach Shock Reflections with Application to Detonation Structure. Master thesis, University of Ottawa (2011)
9. Bourlioux, A., Majda, A.J.: Theoretical and numerical structure for unstable two-dimensional detonations. Combust. Flame **90**, 211–229 (1992)
10. Oran, E.S., Kailasanath, K., Guirguis, R.H.: Numerical simulations of the development and structure of detonations. Prog. Aeronaut. Astronaut. **114**, 155–169 (1998)
11. Gamezo, V.N., Desbordes, D., Oran, E.S.: Formation and evolution of two-dimensional cellular detonations. Combust. Flame **116**, 154–165 (1999)
12. Shepherd, J.E., Pintgen, F., Austin, J.M., Eckett, C.A.: The structure of the detonation front in gases. In: 40th AIAA Aerospace Sciences Meeting, Reno, NV. AIAA paper 2002–0773 (2002)
13. Hu, X.Y., Zhang, D.L., Khoo, B.C., Jiang, Z.L.: The cellular structure of a two-dimensional $H_2/O_2/Ar$ detonation wave. Combust. Theory Model. **8**, 339–359 (2004)
14. Mahmoudi, Y., Mazaheri, K.: High resolution numerical simulation of the structure of 2-D gaseous detonations. Proc. Combust. Inst. **33**, 2187–2194 (2011)
15. Kessler, D.A., Gamezo, V.N., Oran, E.S.: Multilevel detonation cell structures in methane-air mixtures. Proc. Combust. Inst. **33**, 2211–2218 (2011)
16. Williams, D.N., Bauwens, L., Oran, E.S.: Detailed structure and propagation of three-dimensional detonations. Proc. Combust. Inst. **26**, 2991–2998 (1996)
17. Tsuboi, N., Katoh, S., Hayashi, K.: Three-dimensional numerical simulation for hydrogen/air detonation: rectangular and diagonal structures. Proc. Combust. Inst. **29**, 2783–2788 (2002)
18. Eto, K., Tsuboi, N., Hayashi, A.K.: Numerical study on three dimensional C-J detonation waves: detailed propagating mechanism and existence of OH radical. Proc. Comb. Inst. **30**, 1907–1913 (2005)
19. Tsuboi, N., Katoh, S., Hayashi, K.: Detailed structure of spinning detonation in a circular tube. Combust. Flame **149**, 144–161 (2007)
20. Tsuboi, N., Asahara, M., Eto, K., Hayashi, A.K.: Numerical simulation of spinning detonation in square tube. Shock Waves **18**, 329–344 (2008)
21. Tsuboi, N., Hayashi, A.K., Koshi, M.: Energy release effect of mixture on single spinning detonation structure. Proc. Comb. Inst. **32**, 2405–2412 (2009)
22. Deiterding, R.: Parallel Adaptive Simulation of Multi-Dimensional Detonation Structures. University at Cottbus, Ph.D. diss. (2003)
23. He, H.: Numerical Simulations of Unsteady Flows in a Pulse Detonation Engine by the Space-Time Conservation Element and Solution Element Method. The Ohio State University, Ph.D. diss. (2006)
24. Deledicque, V.: Modeling and Simulation of Multidimensional Compressible Flows of Gaseous and Heterogeneous Reactive Mixtures. Ph.D. diss., Universit'e Libre de Bruxelles (2007)
25. Ji, H., Lien, F.S., Yee, E.: A new adaptive mesh refinement data structure with an application to detonation. J. Comput. Phys. **229**(23), 8981–8993 (2010)
26. Dou, H.S., Khoo, B.C.: Effect of initial disturbance on the detonation front structure of a narrow duct. Shock Waves **20**(2), 163–173 (2010)
27. Ji, H., Lien, F.S., Yee, E.: Numerical simulation of detonation using an adaptive Cartesian cut-cell method combined with a cell-merging technique. Comput. Fluids **39**, 1041–1057 (2010)
28. Edwards, D.H., Parry, D.J., Jones, A.T.: The structure of the wave front in spinning detonation. J. Fluid Mech **26**(2), 321–336 (1966)
29. Huang, Y., Tang, H., Li, J., Wang, J.: Deflagration to detonation transition of kerosene-air mixtures in a small-scale pulse detonation engine. Proc. Inst. Mech. Eng. Part G J. Aerosp. Eng. **225**(4), 441–448 (2011)